GEOPHYSICAL RESEARCH LETTERS, VOL. 25, NO. 4, PAGES 445-448, FEBRUARY 15, 1998

TSS-1R vertical electric fields: Long baseline measurements using an electrodynamic tether as a double probe

S.D. Williams[1], B.E. Gilchrist[2], V.M. Agüero[1], R.S. Indiresan[2], D.C. Thompson[3] and W.J. Raitt[3]

Abstract.
This paper presents measurements of vertical electric fields obtained using the Tethered Satellite System (TSS) as an electrodynamic double probe. During five hours of TSS-1R deployment from the space shuttle Columbia in February 1996, observations of induced tether potential were gathered over a baseline from 2 to 20 km in the mid and low latitude F-region ionosphere. The corresponding electric fields derived from the potential measurements are found to be consistent with previous satellite and ground-based measurements for similar ionospheric conditions. The data are unique and demonstrate a new capability for measuring the vertical component of the ionospheric electric field. Comparison of the measured electric field at different tether deployment lengths for corresponding local times reveal that the vertical component of the ambient electric field exists on scales of at least 20 km.

Introduction

The reflight of the Tethered Satellite System (TSS-1R, 2/96) investigated the electrodynamic behavior of a long, insulated wire attached to large charge collecting surfaces at the satellite and the Orbiter [Dobrowolny and Stone, 1994; Stone and Bonifazi, 1997]. Using the Tether Current and Voltage Monitor (TCVM) [Agüero *et al.*, 1994], we obtained an accurate measurement of the induced potential between the points of plasma contact at each end of the deployed tether, which acted as a long electric double probe. In this paper, we present the TCVM measurements of induced tether potential, use those measurements to determine the average vertical component of the ambient electric field, and compare TSS-1R electric field results to previous satellite and ground-based measurements.

While deployed, an electrodynamic tether has several sources of induced potential including the EMF generated by the system's orbital motion through the magnetized ionosphere, naturally occurring ionospheric electric fields, and other natural or man-made electromagnetic wave sources [Banks, 1989; Dobrowolny, 1987; Gilchrist *et al.*, 1995]. Applying the well known derivation of the induced potential across an ionospheric double probe [Mozer, 1973], Williams *et al.* [1996] showed that the tether voltage measurement, V_m, is related to the electric field in the tether frame of reference, $\vec{E}'_T$, and the vector from the Orbiter to the satellite, $\vec{L}$, by $\vec{E}'_T \cdot \vec{L} = V_m + \delta$ where the instrumentation error, δ, is given by

$$\begin{aligned}\delta &= V_m\left(\frac{R_T + R_{Po} + R_{Ps} + R_o + R_s}{R_m}\right) \\ &\quad +(\phi_o - \phi_s) + (WF_s - WF_o).\end{aligned} \tag{1}$$

Here R_m is the resistance over which V_m is measured, R_T is the tether resistance, R_{Pk} is the surface resistance of a tethered end body, R_k is the dynamic resistance of the plasma sheath around a tethered end body, ϕ_k is the potential of a tethered end body relative to the plasma, and WF_k is the surface work function. The subscript (s) refers to the satellite and (o) to the Orbiter.

Using the Lorentz transformation, $\vec{E}'_T = \vec{E}_{amb} + \vec{v_o} \times \vec{B}$, to substitute for $\vec{E}'_T$ and solving for the ambient electric field in the plasma frame, $\vec{E}_{amb}$, along the tether direction, $\hat{L}$, gives

$$\vec{E}_{amb} \cdot \hat{L} = \frac{V_m}{L} - \vec{v_o} \times \vec{B} \cdot \hat{L} + \frac{\delta}{L}, \tag{2}$$

where $\vec{v_o}$ is the Orbiter's velocity in the plasma frame, $\vec{B}$ is the Earth's magnetic field, and δ reduces linearly with increasing tether length. In general, the motional EMF, $\phi_{emf} = \vec{v_o} \times \vec{B} \cdot \vec{L}$ is the main source of induced tether potential. As for all electric field double probes, accurately modeling the motional EMF is critical for measuring the ambient electric field with the electrodynamic tether [Banks, 1989; Hanson *et al.*, 1993].

Measurement

During the TSS-1R mission, the outward deployment and prograde 300 km circular orbit generated a mo-

[1]STAR Laboratory, Stanford Univ., Stanford, CA
[2]Space Phys. Res. Lab., Univ. of Mich., Ann Arbor, MI
[3]Dept. of Physics, Utah State Univ., Logan, UT

Paper number 97GL03259.
0094-8534/98/97GL-03259$05.00

tional EMF which drove electron current from the satellite to the Orbiter. The 1.5 m diameter spherical satellite provided 10 m^2 of conductive surface for plasma contact [Dobrowolny and Stone, 1994]. The Space Shuttle Main Engine (SSME) nozzles provided 70 m^2 of conductive surface at the Orbiter end of the tether [Agüero, 1996]. With the TSS instrumentation configured in high impedance mode, the TCVM measured the potential induced between the satellite skin and the Orbiter's SSME nozzles. Data from periods of low tether circuit impedance or substantial vehicle charging, which would interfere with the measurement of induced tether potential, were omitted.

The uncertainty introduced into the TCVM measurement by the analog high voltage tether circuit and by digital processing was determined by Williams *et al.* [1996]. The sources of analog instrument error are the difference in the *body potentials*, the ratio of the *tether circuit resistances* to the measurement resistance, and the difference in the *work functions* for the two tether ends as shown in Eq. (1). The root-sum-square (RSS) of these sources combined with the calibration uncertainty quantifies the total uncertainty in the TCVM measurement.

The *body potential* of the tethered end bodies for the first TSS mission (TSS-1, August 1992) were predicted by computer simulation based on a detailed current balance for each body [Williams *et al.*, 1996]. The five sources of *tether circuit resistance* were determined by measurement and numerical analysis. The sheath resistances were derived from the simulation results. Thompson *et al.* [1997] estimated the tether resistance from the satellite current-voltage response. The plasma contact resistance of the Inconel-718 SSME nozzles is assumed to be negligible. The plasma contact resistance of the RM400 paint on the satellite's exterior was measured [Carruth, 1995]. While the *work function* of the RM400 paint is not yet available, the difference in work function between the satellite paint and the Orbiter engine nozzles could be as much as several eV based on a comparison with similar conductive materials. Because the work functions do not vary with trajectory, the dominant effect introduced into the potential measurement should be a d.c. offset [Hanson *et al.*, 1993]. Any variation resulting from attitude, surface contamination or temperature during the five hours of the tether deployment is expected to be less than 10% [Jenkins and Trodden, 1965]. Temperature compensated *calibrations* were developed for the three gain states of the TCVM using data from plasma chamber tests [Indiresan, 1995].

The large surface areas for plasma contact at the satellite and the Orbiter reduced the instrumentation error, δ, by minimizing the plasma resistance ($\approx$20-120 Ω) and body potentials (0.2 to 0.7 V). The total measurement uncertainty of 2 V was dominated by the uncertainty in the x1 gain state calibration used for tether deployed lengths of more than 5 km (Table 1).

To find the ambient electric field, we developed a numerical model of the motional EMF using the *velocity* of the tether in the co-rotating frame of reference, the *magnetic field*, and the *geometry* of the plasma contact points at the Orbiter and satellite ends of the tether. The Orbiter ephemeris is provided in the Postflight Attitude and Trajectory History (PATH) [Rockwell, 1996a]. The inertial position and velocity provided by PATH were used to calculate the *velocity* with respect to the co-rotating frame. The *magnetic field* is determined using the 1995 International Geomagnetic Reference Field (IGRF) [Barton, *et al.*, 1996] and not the Tether Magnetic Field Experiment (TEMAG) satellite-based magnetometer measurements because the attitude of the TSS-1R satellite is not sufficiently well known. IGRF accuracy for the relatively quiet ionospheric conditions of TSS-1R was estimated to be 180 nT in magnitude and 380 nT in direction [Williams *et al.*, 1996]. The *geometry* is determined from the Relative Best Estimate of Trajectory (RELBET) data [Rockwell, 1996b] which has an angular standard deviation of 0.02 radians and a relative position standard deviation of 50 m (at 18,300 m). The resulting motional EMF model has a derived accuracy of 1% as shown in Table 1, which is equivalent to $\approx$16 V at 10 km. The principal contributors to the model uncertainty are the magnitude uncertainty in the IGRF magnetic field and the angular uncertainty of the RELBET derived separation vector, $\vec{L}$.

Table 1. Uncertainty in tether potential measurement, Motional EMF model, and measured electric field.

Quantity	Uncertainty Volts[1]	mV/m[2]
Voltage Measurement[3]	2.0	0.2
Motional EMF Model	16.4	1.6
Electric Field Measurement	16.5	1.6

[1]Uncertainty at the mean tether potential of -1653 V.
[2]Uncertainty at the mean separation distance of 10,092 m.
[3]x10 gain used before 056/22:56 GMT has uncertainty 0.29 V, x1 gain used thereafter has uncertainty 2.02 V.

The numerical model of motional EMF was used with the TCVM measurement and Eq. (2) to calculate the ambient electric field along the tether, $\vec{E}_{\rm amb} \cdot \hat{L}$. The accuracy of the resulting electric field measurement is determined by the RSS of the measurement and model uncertainties, with the result normalized over the mean separation distance, $\bar{L}$. The long baseline of the deployed tether substantially attenuated the uncertainty in the measured electric field caused by instrumentation error, δ, and the motional EMF model uncertainty. For TSS-1R, the integrated ambient electric field measurement has an uncertainty of 1.6 mV/m.

Results

The TSS-1R deployment began with satellite flyaway at 056/20:45 GMT and ended at 057/01:29 GMT with the tether break at 19.7 km. Figure 1 shows a com-

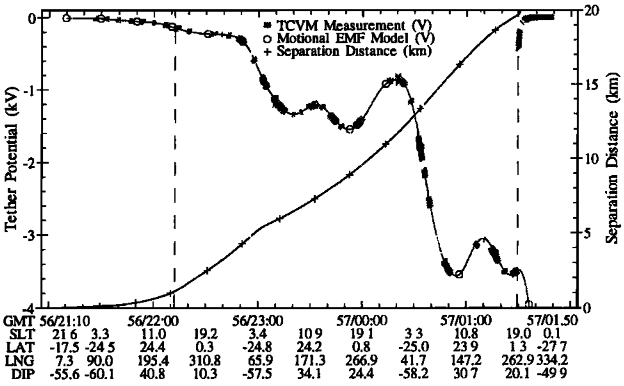

Figure 1. Comparison of TCVM tether potential measurement with modeled motional EMF, and the separation distance, L, for TSS-1R. Vertical dashed lines identify the data range used for ambient electric field analysis. Data from periods of active modes of tether circuit instruments, Orbiter thruster firings, and telemetry corruption were excluded.

parison of the measured tether voltage to the modeled motional EMF. Data from active, low impedance periods are excluded, leaving ≈ 30% of the more than 16,000 TCVM measurements for use in the analysis. The modeled values of motional EMF are within 3.8% of the TCVM measurements over the range of -108 V to -3569 V.

Figure 2 shows the integrated ambient electric field measurements for TSS-1R. The basic source of electric fields in the low latitude F-region ionosphere are tidally driven neutral winds [Fejer, 1991; Coley *et al.*, 1994; Maynard *et al.*, 1995]. We have included in Figure 2 the ambient electric field along the tether predicted using neutral winds as a proxy for plasma drift as given by $\vec{E}_{\text{drift}} \cdot \hat{L} = -\vec{v}_{\text{p}} \times \vec{B} \cdot \hat{L}$, where the neutral wind velocity, $\vec{v}_{\text{p}}$, predicted by the Hedin Wind Model (HWM) [Hedin *et al.*, 1996] and the IGRF magnetic field, $\vec{B}$, are calculated at the Orbiter. The character of the measured ambient electric field is strikingly

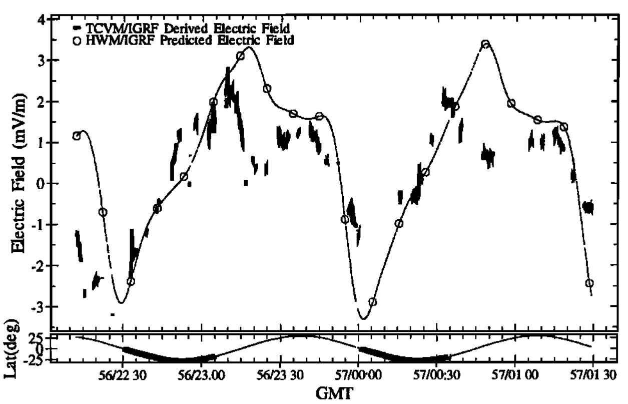

Figure 2. TSS-1R *ambient electric field*, $\vec{E}_{\text{amb}} \cdot \hat{L}$, derived as the difference of measured tether potential and modeled motional EMF divided by separation distance, L. Lower panel shows TSS latitude with thick curve indicating local night.

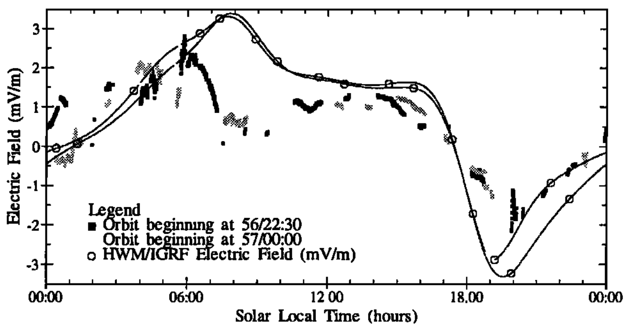

Figure 3. TSS-1R *ambient electric field*, $\vec{E}_{\text{amb}} \cdot \hat{L}$, versus solar local time for two successive orbits with an order of magnitude variation in tether length.

similar to the HWM based predictions during the local night with a structure that repeats over intervals matching the 90 minute orbital period. Beginning with the southward equatorial crossing into local night at 56/22:30 GMT and again at 57/00:00 GMT, the measured values rise from local minima to pre-dawn peaks. This correlation is expected since F-region neutral wind driven polarization fields are a significant source of nighttime F-region electric fields [Fejer, 1991]. Figure 3 shows the electric field data and the HWM based predictions for the last two orbits of tether deployment plotted against solar local time. Both orbits show upward post-noon electric field and have values which vary over approximately ±3 mV/m, consistent with low latitude and altitude electric field measurements from Dynamics Explorer 2 (DE-2) [Hanson *et al.*, 1993].

The character of the TSS-1R average electric field is also similar to San Marco D measurements for local times of 1200 to 2200 [Maynard *et al.*, 1995]. For local times of 2200 to 1200 the San Marco D values reflect a minimum of up to -6 mV/m whereas the TSS-1R values indicate a positive electric field. This divergence may in part be explained by the inclination of the respective orbits with San Marco D nearly equatorial (2.9°) and TSS-1R reaching mid-latitudes (-28.5°) near local midnight. An analysis of mid-latitude DE-2 zonal ion drift data by Heelis and Coley [1992] showed that for the Kp consistent with TSS-1R (≈ 25 [Dept. of Commerce, 1996]) the equivalent electric field is positive in the post-midnight region reaching a maximum around 0600 local time, similar to the TSS-1R data. Fejer performed a comparison of DE-2 data with ground based radar measurements from Jicamarca, Arecibo, and Shigaraki [Fejer, 1991]. The Jicamarca and Arecibo data both match the TSS-1R measurements for the post-noon to midnight period. The MU radar measurements from Shigaraki contain the same local minimum at ≈0800 local time as the TSS-1R data, which were measured at approximately the same longitude (≈135°E). In a further analysis of Arecibo plasma drifts, Fejer finds that the MU radar results are similar to DE-2 average zonal drifts, in that both contain peaks at 0600 and 1300 local time, which are missing from the Arecibo data [Fejer, 1993], but are similar to the TSS-1R results.

We therefore conclude that the magnitude and character of the TSS-1R measurements of the vertical component of the F-region electric field are consistent with previous satellite and ground-based measurements. Furthermore, the similarity of the measured electric field over two succeeding orbits, which had an order of magnitude variation in deployed tether length, strongly suggests that the electric field measured by TSS-1R existed on scales of at least 20 km.

Future research to refine the electric field measurement will include performing the body potential and sheath resistance simulation for the TSS-1R trajectory to further evaluate plasma gradient effects. Incorporating variations in velocity and magnetic field over the length of the tether and the use of TEMAG magnetic field measurements could improve the accuracy of the motional EMF model and the TSS-1R electric field measurements. These results show that gravity gradient stabilized tethers provide a new technique for high resolution measurement of large scale ionospheric electric fields. By placing differential GPS receivers [Gilchrist *et al.*, 1995] and magnetometers at each end, the motional EMF model accuracy could be improved, resulting in electric field measurement uncertainties as low as 0.3 mV/m for a 20 km tether.

Acknowledgments.
This work was funded by NASA under contract NAS8-39381 to the University of Michigan and was produced in partial fulfillment of the requirements for a Ph.D. in Aeronautics and Astronautics by the principal author, S. Williams. The authors express gratitude for the support provided by M. Gallagher; the contributions of P.M. Banks, P.R. Williamson, D. Lauben, A.B. White, L. Allen, I. Linscott, J. Bryan, C. Gronbeck, J. Burr, V. Tolat and L. Clarke during the development of the TCVM; and for the efforts of L. Liebler, S. Bilén, D. Morris and N. Voronka during the reflight.

References

Agüero, V.M., P.M. Banks, B.E. Gilchrist, I.R. Linscott, W.J. Raitt, D.C. Thompson, V.V. Tolat, A.B. White, S.D. Williams, and P.R. Williamson, The shuttle electrodynamic tether system (SETS) on TSS-1, *Il Nuovo Cimento, 17C,* 49, 1994.

Agüero, V.M., *A Study of Electrical Charging on Large LEO Spacecraft Using a Tethered Satellite as a Remote Plasma Reference*, Ph.D. Diss., Stanford Univ., June 1996.

Banks, P.M., Review of electrodynamic tethers for space science, *J. Spacecr. Rockets, 26,* 234, 1989.

Carruth, M.R., TSS conductive coating studies, Fourth TSS-1R IWG, MSFC Matl. & Proc. Lab., Feb. 1995.

Barton, C.E. *et al.,* International geomagnetic reference field, 1995 revision, *Pure Appl. Geophys., 147,* 195, 1996.

Coley, W.R., R.A. Heelis, and N.W. Spencer, Comparison of low-latitude ion and neutral zonal drifts using DE 2 data, *J. of Geophys. Res., 99,* 341, 1994.

Dobrowolny, M. and N.H. Stone, A technical overview of TSS-1: the first tethered satellite system mission, *Il Nuovo Cimento, 17C,* 1, 1994.

Dobrowolny, M., Electrodynamics of long metallic tethers in the ionospheric plasma, *Radio Sci., 13,* 417, 1987.

Fejer, B.G., Low latitude electrodynamic plasma drift: A review, *J. Atmos. Terr. Phys., 53,* 677, 1991.

Fejer, B.G., F region plasma drifts over arecibo: Solar cycle, seasonal, and magnetic activity effects, *J. Geophys. Res., 98,* 13645, 1993.

Gilchrist, B.E., S.D. Williams, N. Voronka, W.J. Raitt, D.C. Thompson, S.G. Bilén, and V.M. Agüero, Space tethers for double probe potential measurements in the ionosphere and magnetosphere, *AGU Chapman Conference*, Santa Fe, NM, Apr. 1995.

Hanson, W.B., W.R. Coley, R.A. Heelis, N.C. Maynard, and T.L. Aggson, A comparison of in situ measurements of E and -VxB from Dynamics Explorer 2, *J. Geophys. Res., 98,* 21501, 1993.

Hedin, A.E., *et al.,* Empirical wind model for the upper, middle and lower atmosphere, *J. Atmos. Terr. Phys., 58,* 1421, 1996.

Heelis, R.A. and W.R. Coley, East-west ion drifts at mid-latitudes observed by Dynamics Explorer 2, *J. Geophys. Res., 97,* 19461, 1992.

Indiresan, R., TVMDC360 calibration, Tech. Report 057-0514, Space Phys. Res. Lab., Univ. of Michigan, 1995.

Jenkins, R.O., and W.G. Trodden, *Electron and Ion Emission from Solids*, Dover Publications, New York, 1965.

Maynard, N.C., T.L. Aggson, F.A. Herrero, M.C. Liebrecht, and J.L. Saba. Average equatorial zonal and vertical ion drifts determined from San Marco D electric field measurements. *J. Geophys. Res., 100,* 17465, 1995.

Mozer, F.S., Analyses of techniques for measuring DC and AC electric fields in the magnetosphere, *Space Sci. Reviews, 14,* 272, 1973.

Rockwell Space Operations Co., STS-75 PATH final report, NASA, Houston, TX, 1996.

Rockwell Space Operations Co., STS-75 RELBET final report, NASA, Houston, TX, 1996.

Solar-geophysical data, Dept. of Commerce, Nat. Geophys. Data Center, Boulder CO, Apr. 1996.

Stone, N. and C. Bonifazi, The TSS-1R mission: Overview and scientific context, *Geophys. Res. Lett., this issue,* 1997.

Thompson, D.C., B.E. Gilchrist, C. Bonifazi, S.D. Williams, W.J. Raitt, J.-P. Lebreton, and W.J. Burke, The current voltage characteristics of a large probe in low earth orbit: TSS-1R results, *Geophys. Res. Lett., this issue,* 1997.

Williams, S.D., B.E. Gilchrist, V.M. Agüero, D.C. Thompson, W.J. Raitt, S. Orsini, and R.S. Indiresan, Tether potential measurements and models for TSS-1, Tech. Report STR025, Stanford Univ., Dec. 1996.

V. Agüero and S. Williams, STARLAB, Stanford Univ., Stanford, CA 94305-9515. (email: scott@nova.stanford.edu)

B. Gilchrist and R. Indiresan, SPRL, 2455 Hayward St., Univ. of Michigan, Ann Arbor, MI 48109-2143.

W. J. Raitt and D. Thompson, CASS, Utah State Univ., Logan, UT 84322-4055.

(Received January 23, 1997; revised October 15, 1997; accepted October 28, 1997.)